Sensor and Body Frames Rotation Calibration Through Attitude Restriction ⋆

Conrado S. Miranda * **Janito V. Ferreira** *

* *School of Mechanical Engineering, University of Campinas, Brazil*
(e-mail:{cmiranda,janito}@fem.unicamp.br)

Abstract: This paper describes an algorithm to calibrate the misalignment between sensor and body frames using only estimates of user-chosen attitudes. The focus is on the reduction of requirements, such as precise positioning, without introducing errors, so that any user without auxiliary equipment can calibrate a system. The greedy algorithm proposed is able to correctly calibrate the rotation in most cases, with the error median below the noise median, and the conditions where it may not work are discussed and a solution presented.

Keywords: Attitude; Calibration; Rotation; Sensor; State estimation

1. INTRODUCTION

The sensor reading is an important phase during the filtering step in a robot's control loop. Although state estimation algorithms usually assume that the readings occur in a particular frame, e.g. Elkaim et al. (2012); Gebre-Egziabher et al. (2000); Thrun et al. (2005); Schopp et al. (2010), called the body frame, that may not be true because of misalignments due to sensors calibration and placement. If the difference between the sensor frame, where the readings really occur, and the body frame isn't taken into account, the states estimates may become incorrect and cause the system to fail.

An algorithm to calibrate the misalignment between two three-axis sensors, whose sensed unit vectors are known in the inertial frame and can be measured in the body frame, was introduced in Elkaim (2013). The problem is posed as a Wahba's problem, see Shuster (2006), and its solution is a rotation matrix that transforms readings from the second sensor to readings in the same frame used by the first sensor, eliminating the misalignment. When sensors can be grouped to produce 3D points, the generic framework described in Le and Ng (2009) can be used to calibrate sensors' parameters and frames of reference by matching the information captured by each group. Although all these techniques allow sensors to work on the same frame of reference, they provide a sensor frame that may still be misaligned with the desired body frame.

Due to the polar decomposition theorem, as described in Alonso and Shuster (2002), the calibration algorithms aren't able to distinguish between the body's current attitude and the misalignment between sensor and body frame. Therefore, the calibration must be performed in a specific frame of reference, which may be different from the body one. In the case of field sensors, a solution provided by Vasconcelos et al. (2011) is to use another sensor, which has already been calibrated to match the body frame, to measure the field at the same orientations that the

new sensor is placed. Comparing the readings, a rotation matrix can be found to transpose the readings from the sensor to the body frame. Although this method correctly solves the problem, it depends on another pre-calibrated sensor, which may not be available, and may propagate calibration errors from one sensor to another. Another solution is to pre-define the samples' orientations so that correct body attitude is known. However, this method requires the user to be precise during calibration, which may require tools not available or restrict the number of orientations that can be achieved.

The algorithm presented in this paper proposes a solution to the problem of finding the rotation between the sensor and body frame without additional sensors. Furthermore, the algorithm must be easy to use, so that a layman can follow the steps needed. This requirement is often ignored, but the calibration performed at the vendors may become incorrect due to incorrect transportation or usage, and it must be redone by the user. The algorithm is a generalization and relaxation of the pre-defined orientations method previously described, and uses attitude estimates computed by another algorithm, such as those proposed by Gebre-Egziabher et al. (2000); Sabatini (2006); Madgwick et al. (2011); Mahony et al. (2008); Batista et al. (2009), at attitudes constructed in a restricted way, while providing the user freedom to choose the exact positioning. This work is an improvement of the authors' previous algorithm, introduced in Miranda and Ferreira (2013), to reduce restrictions and improve robustness, and these two are, to the best of the authors' knowledge, the only algorithms to perform this calibration without external references or enforcing specific system positioning.

This paper is organized as follows: Section 2 describes the reference frames, their relation and how to capture the attitude estimates. Based on data capture methodology, Section 3 formulates an optimization problem for the calibration, stating how it is decomposed and solved, while Section 4 presents an overview of the calibration algorithm that performs the optimization. Section 5 presents the algorithm's test through simulation, as the authors currently
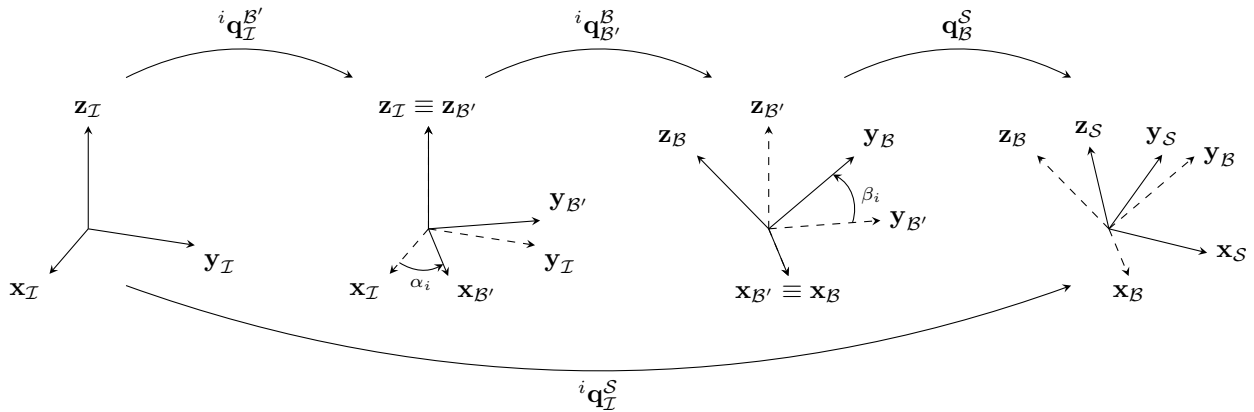
Fig. 1. Example of attitude decomposition with $d(i) = \mathbf{x}$ and $s(i) = +1$, showing how the body frame $\mathcal{B}$ must be positioned with respect to the inertial frame $\mathcal{I}$ used by the attitude estimation algorithm.

lack the required equipment, and an analysis of the results. Finally, Section 6 provides concluding remarks and future research directions.

2. DATA CAPTURE

The algorithm described in this paper uses attitude estimates collected at restricted orientations to calibrate the rotation between body and sensor frame. To properly describe these orientations, first the frames of reference and their relations must be defined. Figure 1 shows an example of a correctly collected estimate, which can be used as a guide to how the frames must be related. The idea is that, while a full 3D arbitrary orientation can't be distinguished from the misalignment, a rotation with 2 degrees of freedom instead of 3 and some other information provide enough data to reconstruct the orientation used.

The fixed inertial frame $\mathcal{I}$, defined by the attitude estimation algorithm, and the intermediate body frame $\mathcal{B}'$ differ only by a rotation around the shared coordinate direction $\mathbf{z}$. Each attitude estimate is then collected at the true body frame $\mathcal{B}$, which differs from $\mathcal{B}'$ by a rotation around a local basis vector, chosen by the user. Note that $\mathcal{B}'$ is introduced so that $\mathcal{B}$ can be described by 2 rotations from $\mathcal{I}$ using only the basis vectors as axis. This also makes it clear that, for this algorithm, $\mathcal{B}$ must follow a rule that limit its positioning, as an arbitrary rotation would require 3 rotations around basis vectors. Finally, the sensor frame $\mathcal{S}$, where all the measurements are made, differs from $\mathcal{B}$ by an unknown fixed rotation. It must be highlighted that more general rotations between the frames can be used by creating intermediary frames, as long as the alignments are known, and not all rotations need to be performed, so that the respective angles are null. For instance, the pre-defined orientation alignment method can be described by a known rotation between $\mathcal{I}$ and $\mathcal{I}'$ and no further body rotation, defining $\mathcal{I}' = \mathcal{B}' = \mathcal{B}$.

As the attitude estimation algorithm is only aware of the inertial frame $\mathcal{I}$, used as a reference, and the sensor frame $\mathcal{S}$, in which the sensors were calibrated, each attitude estimate represents a rotation from $\mathcal{I}$ to $\mathcal{S}$, which can be written as the quaternion ${}^{i}\mathbf{q}_{\mathcal{I}}^{\mathcal{S}}$. Using the frames described previously, these attitudes can be written as

$$ {}^{i}\mathbf{q}_{\mathcal{I}}^{\mathcal{S}} = \mathbf{q}_{\mathcal{B}}^{\mathcal{S}} \otimes {}^{i}\mathbf{q}_{\mathcal{B}'}^{\mathcal{B}} \otimes {}^{i}\mathbf{q}_{\mathcal{I}}^{\mathcal{B}'} \tag{1} $$

where $\mathbf{q}_{\mathcal{B}}^{\mathcal{S}}$ is the rotation between the body and sensor frame, shared by all samples, ${}^{i}\mathbf{q}_{\mathcal{B}'}^{\mathcal{B}}$ is the rotation between the intermediate body frame and the real body frame, ${}^{i}\mathbf{q}_{\mathcal{I}}^{\mathcal{B}'}$ is the rotation between the fixed inertial frame and the intermediate body frame, and $\otimes$ is the quaternion product operator.

As a quaternion can be described by a vector and an angle, the notation for this format used in this paper is given by

$$ \mathbf{q}_{\alpha,\mathbf{v}} := \cos\left(\frac{\alpha}{2}\right) + \mathbf{v}\sin\left(\frac{\alpha}{2}\right). \tag{2} $$

where α is the rotation performed around $\mathbf{v}$.

Using this notation, the quaternions with specific directions can be rewritten as ${}^{i}\mathbf{q}_{\mathcal{I}}^{\mathcal{B}'} = \mathbf{q}_{\alpha_i,\mathbf{z}}$ and ${}^{i}\mathbf{q}_{\mathcal{B}'}^{\mathcal{B}} = \mathbf{q}_{\beta_i,d(i)}$, where $\alpha_i, \beta_i \in [-\pi, \pi)$ are the rotation angles and $d(i)$ is the rotation direction for the i-th sample. Note that $d(i)$ may assume values $\mathbf{x}$, $\mathbf{y}$ or $\mathbf{z}$, but the last one is redundant since ${}^{i}\mathbf{q}_{\mathcal{I}}^{\mathcal{B}'}$ already describes a rotation in that direction. Therefore, one can fix $\beta_i = 0$ when $d(i) = \mathbf{z}$ and let α_i describe the rotation, thus avoiding a continuous subspace of solutions that could decrease the algorithm's performance. Additionally, due to the multiplicity of solutions, which is clear when the mirroring of all axis is considered, the sign of the rotation β_i around $d(i)$ must be provided. Such information is given to the algorithm through a function $s(i) = \text{sign}(\beta_i)$.

3. OPTIMIZATION PROBLEM

An appropriate formulation for the quaternion averaging problem is given by Markley et al. (2007), where the problem is defined by finding the solution $\hat{\mathbf{q}}$ to the optimization

$$ \min_{\mathbf{q} \in \mathbb{S}^3} \sum_{i=1}^{n} w_i \|R(\mathbf{q}) - R(\mathbf{q}_i)\|_F^2 \tag{3} $$

where $R(\cdot)$ is the rotation matrix defined by its argument, $\|\cdot\|_F$ is the Frobenius norm, and w_i is the weight associated with the uncertainty of the i-th sample $\mathbf{q}_i$. This problem can be rewritten as

$$ \max_{\mathbf{q} \in \mathbb{S}^3} \mathbf{q}^T \mathbf{M} \mathbf{q}, \quad \mathbf{M} = \sum_{i=1}^{n} w_i \mathbf{q}_i \mathbf{q}_i^T \tag{4} $$

and its solution is given by the eigenvector of $\mathbf{M}$ associated with the maximum eigenvalue.

Based on Eq. (3), the problem of estimating the quaternions defined in Eq. (1) can also be posed as an optimization problem. Let $\{^i\mathbf{q}_{\mathcal{I}}^{\mathcal{S}}\}$ be a set of n attitudes collected by the method described in the Sec. 2. The optimization problem tries to reconstruct the samples and is given by:

$$\min_{\substack{\mathbf{q}_{\mathcal{B}}^{\mathcal{S}} \in \mathbb{S}^3 \\ \alpha_i, \beta_i \in [-\pi, \pi)}} \sum_{i=1}^{n} w_i \left\| R(^i\mathbf{q}_{\mathcal{I}}^{\mathcal{S}}) - R(\mathbf{q}_{\mathcal{B}}^{\mathcal{S}} \otimes {}^i\mathbf{q}_{\mathcal{B}'}^{\mathcal{B}} \otimes {}^i\mathbf{q}_{\mathcal{I}}^{\mathcal{B}'}) \right\|_F^2$$

$$\text{subject to} \quad s(i)\beta_i \geq 0$$
$$d(i) = \mathbf{z} \Rightarrow \beta_i = 0$$
$$^i\mathbf{q}_{\mathcal{B}'}^{\mathcal{B}} = \mathbf{q}_{\beta_i, d(i)}$$
$$^i\mathbf{q}_{\mathcal{I}}^{\mathcal{B}'} = \mathbf{q}_{\alpha_i, \mathbf{z}}$$

$$(5)$$

where $s(i)$ is the sign and $d(i)$ is the direction given by the user for the i-th sample.

The optimization problem doesn't have a direct closed-form solution and optimizing all variables simultaneously would be too expensive while possibly providing poor performance. However, each quaternion by itself has a closed-form solution, as they can be written in a similar fashion to Eq. (4). Therefore, they'll be optimized individually using a greedy algorithm, that is, one quaternion is estimated while the other are considered fixed. The next sections describe how each one is optimized.

It's important to highlight that this cost function depends on many parameters other than the desired $\mathbf{q}_{\mathcal{B}}^{\mathcal{S}}$, due to the flexibility allowed for the rotations. This not only increases the optimization complexity, but may also increase the number of local minima, possibly resulting in poorer results. Moreover, a good reconstruction, which is the objective of the proposed cost function, doesn't always leads to a good value for $\mathbf{q}_{\mathcal{B}}^{\mathcal{S}}$. However, there's no way to measure the calibration objective directly, so this indirect method must be used.

3.1 $\mathbf{q}_{\mathcal{B}}^{\mathcal{S}}$ estimation

Considering every quaternion except for $\mathbf{q}_{\mathcal{B}}^{\mathcal{S}}$ as fixed in Eq. (5), the problem can be rewritten as:

$$\min_{\mathbf{q}_{\mathcal{B}}^{\mathcal{S}} \in \mathbb{S}^3} \sum_{i=1}^{n} w_i \left\| R(\mathbf{q}_{\mathcal{B}}^{\mathcal{S}}) - R(^i\mathbf{q}_{\mathcal{I}}^{\mathcal{S}} \otimes (^i\mathbf{q}_{\mathcal{B}'}^{\mathcal{B}} \otimes {}^i\mathbf{q}_{\mathcal{I}}^{\mathcal{B}'})^{-1}) \right\|_F^2$$

which has the same form as Eq. (3). Therefore, it can be rewritten as Eq. (4) and its solution is given by the eigenvector associated with the maximum eigenvalue of the matrix $\mathbf{M}$ built using the equation above.

3.2 $^i\mathbf{q}_{\mathcal{B}'}^{\mathcal{B}}$ estimation

Consider now that every quaternion except for $^i\mathbf{q}_{\mathcal{B}'}^{\mathcal{B}}$ is fixed in Eq. (5). In this case, the algorithm still has restrictions that must be satisfied. To solve it, the problem will be relaxed, and the solution will be transformed into a valid solution to the original problem. Note that, if $d(i) = \mathbf{z}$, this estimation is ignored since β_i must be zero, as described earlier.

Although the relaxed problem is similar to the one given by Eq. (3), the sum has only one term. This simplifies the

solution, which is given by simply equating the quaternions describing the rotations:

$$^i\tilde{\mathbf{q}}_{\mathcal{B}'}^{\mathcal{B}} = (\mathbf{q}_{\mathcal{B}}^{\mathcal{S}})^{-1} \otimes {}^i\mathbf{q}_{\mathcal{I}}^{\mathcal{S}} \otimes (^i\mathbf{q}_{\mathcal{I}}^{\mathcal{B}'})^{-1}, \qquad (6)$$

where $^i\tilde{\mathbf{q}}_{\mathcal{B}'}^{\mathcal{B}}$ is the relaxed quaternion.

The first problem from the relaxation is defining how to get $^i\mathbf{q}_{\mathcal{B}'}^{\mathcal{B}}$, which only rotates around $d(i)$, from the general quaternion $^i\tilde{\mathbf{q}}_{\mathcal{B}'}^{\mathcal{B}}$. Let $\mathbf{q}$ be a quaternion, whose vector form can be written as $\mathbf{q} = [q_0, q_1, q_2, q_3]^T$. Without loss of generality, the rotation described by $\mathbf{q}$ can be decomposed in a rotation around the $\mathbf{z}$ axis, named $\mathbf{q}_z = [q_{z,0}, 0, 0, q_{z,3}]^T$, and a rotation around a vector on the xy plane, named $\mathbf{q}_{xy} = [q_{xy,0}, q_{xy,1}, q_{xy,2}, 0]^T$, so that $\mathbf{q} = \mathbf{q}_{xy} \otimes \mathbf{q}_z$. The quaternion product can be written as the following system of linear equations:

$$\begin{aligned} q_0 &= q_{xy,0}q_{z,0} \\ q_1 &= q_{xy,1}q_{z,0} + q_{xy,2}q_{z,3} \\ q_2 &= q_{xy,2}q_{z,0} - q_{xy,1}q_{z,3} \\ q_3 &= q_{xy,0}q_{z,3} \end{aligned} \qquad (7)$$

If $q_0 \neq 0$ or $q_3 \neq 0$, then $\mathbf{q}_z$ can be built from a non-normalized quaternion $\tilde{\mathbf{q}}_z = [q_0, 0, 0, q_3]^T$ such that $\mathbf{q}_z = \tilde{\mathbf{q}}_z / \|\tilde{\mathbf{q}}_z\|$. If $q_0 = q_3 = 0$, then the rotation angle for $\mathbf{q}$ is given by $\theta = \pi + 2k\pi, k \in \mathbb{Z}$ and the direction $\mathbf{v}$ doesn't have any component in the $\mathbf{z}$ direction, according to Eq. (2). This means that the resulting rotation given by $\mathbf{q}$ only express a rotation around a vector in the xy plane, even if a rotation around $\mathbf{z}$ occurred before. Therefore, the information about the rotation around $\mathbf{z}$ is lost and any value can be chosen here, as all of them produce consistent results. In this case, the previous estimate is kept.

This method of extracting a rotation around a single axis from a general 3D rotation is similar for all directions aligned with coordinates axis, although only the case for $\mathbf{z}$ was shown. Hence the estimate of $^i\mathbf{q}_{\mathcal{B}'}^{\mathcal{B}}$ is obtained from $^i\tilde{\mathbf{q}}_{\mathcal{B}'}^{\mathcal{B}}$ using the direction $d(i)$ and a system of equations similar to Eq. (7).

Once the estimate has only the desired components, the sign constraint given by

$$s(i)\beta_i \geq 0$$

must be satisfied. If it's not already satisfied, there are two methods to correct the estimate.

The first one is using the null quaternion $\mathbf{q}_{0,d(i)}$, which satisfies the constraint, but provides no information to the algorithm about the axis direction. The second method, chosen to be used in this paper, changes the sign of β_i, which corresponds to changing the sign of the quaternion's scalar term. Although this change may increase the cost function more than using the null quaternion, the information provided is beneficial.

Although it may seem obvious at first that assuming no rotation is better than assuming a wrong one, it limits the algorithm's exploration. With no information about the direction $d(i)$, the quaternion $^i\mathbf{q}_{\mathcal{I}}^{\mathcal{B}'}$ can rotate the coordinate system to whatever orientation provides the best result, with no regard about the actual orientation for the i-th sample. This hypothesis was confirmed during tests, where using the null quaternion made the algorithm converge to worse local minima than the alternative.

Additionally, the incorrect sign in the relaxed solution comes from noise in the attitude estimate in the regions where β_i changes sign, namely close to 0 and π. As this noise usually is small compared to the range of values available, the solution with correct sign is close to the relaxed one, creating a small increase in the cost described by Eq. (5). However, as will be shown in Sec. 5.2, this small change may have drastic affects on the result if ignored by the user during data collection.

3.3 $^i\mathbf{q}_{\mathcal{I}}^{\mathcal{B}'}$ estimation

This estimation step is similar to the one described in the previous section, except that the rotation is always performed around the **z** axis and there's no sign constraint. Hence it is solved by finding a relaxed solution similar to Eq. (6), and extracting the scalar and **z** vector components, respectively q_0 and q_3.

4. CALIBRATION ALGORITHM

Using each estimation problem defined in Sec. 3, a greedy calibration algorithm can be defined as shown in Alg. 1. However, not every step reduces the cost function, so there is no guarantee that it will converge. Hence the argument IT is introduced to the algorithm to specify the maximum number of iterations possible.

Algorithm 1 Rotation estimation between $\mathcal{B}$ and $\mathcal{S}$

> **procedure** CALIBRATION($\{^i\hat{\mathbf{q}}_{\mathcal{I}}^{\mathcal{S}}\}, d(\cdot), s(\cdot), \text{IT}$)
> $\hat{\mathbf{q}}_{\mathcal{B}}^{\mathcal{S}} \leftarrow \mathbf{q}_{0,\mathbf{z}}$
>   **for** $i \leftarrow 1$ **to** n **do**
> $^i\hat{\mathbf{q}}_{\mathcal{B}'}^{\mathcal{B}} \leftarrow \mathbf{q}_{0,\mathbf{z}}$
> 5: $^i\hat{\mathbf{q}}_{\mathcal{I}}^{\mathcal{B}'} \leftarrow \mathbf{q}_{0,\mathbf{z}}$
>   **end for**
>   **repeat**
>   Estimate $\hat{\mathbf{q}}_{\mathcal{B}}^{\mathcal{S}}$ using Sec. 3.1
>   **for** $i \leftarrow 1$ **to** n **do**
> 10:   **if** $d(i) \neq \mathbf{z}$ **then**
>   Estimate $^i\hat{\mathbf{q}}_{\mathcal{B}'}^{\mathcal{B}}$ using Sec. 3.2
>   **end if**
>   Estimate $^i\hat{\mathbf{q}}_{\mathcal{I}}^{\mathcal{B}'}$ using Sec. 3.3
>   **end for**
> 15:   IT $\leftarrow$ IT $- 1$
>   **until** convergence **or** IT $= 0$
>   **return** $\hat{\mathbf{q}}_{\mathcal{B}}^{\mathcal{S}}$
> **end procedure**

---

5. SIMULATION

The simulation performed for this paper consists of noisy synthetic data to assess the algorithm's performance for many sets of attitude estimates. No experimental results with real sensors are provided because, at the time of writing, the authors didn't have access to the equipment required.

5.1 Synthetic data

A total of 1000 Monte Carlo runs were performed to evaluate the algorithm's performance, and IT was set to

Table 1. Simulation parameters

Parameter	Description	Value
m	Number of attitudes for each axis	
$\mathbf{q}_{\mathcal{B}}^{\mathcal{S}}$	Rotation between frames	See Eq. (8)
α_i	Rotation angle for $^i\mathbf{q}_{\mathcal{I}}^{\mathcal{B}'}$	$\mathcal{U}\left([-\pi,\pi)\right)$
β_i	Rotation angle for $^i\mathbf{q}_{\mathcal{B}'}^{\mathcal{B}}$	$\mathcal{U}\left(I_\beta\right)$
γ	Estimates' noise level	
	Total of Monte Carlo runs	1000

1000, as at that point all runs had either converged or started oscillating in the neighborhood of a single point due to the non-minimizing changes in β_i.

For each Monte Carlo run, the quaternion $\mathbf{q}_{\mathcal{B}}^{\mathcal{S}}$ was created according to the method described in Kuffner (2004), which is given by:

$$s, p_1, p_2 \sim \mathcal{U}\left([0,1]\right)$$
$$\sigma_1 = \sqrt{1-s}, \quad \sigma_2 = \sqrt{s}$$
$$\theta_1 = 2\pi p_1, \quad \theta_2 = 2\pi p_2 \tag{8}$$
$$\mathbf{q} = [\sigma_2 \cos\theta_2, \sigma_1 \sin\theta_1, \sigma_1 \cos\theta_1, \sigma_2 \sin\theta_2]^T$$

where $\mathcal{U}(\cdot)$ is the uniform distribution. The quaternions $^i\mathbf{q}_{\mathcal{I}}^{\mathcal{B}'}$ were given by $\mathbf{q}_{\alpha_i,\mathbf{z}}$, where $\alpha_i \sim \mathcal{U}\left([-\pi,\pi)\right)$, while $^i\mathbf{q}_{\mathcal{B}'}^{\mathcal{B}}$ were given by $\mathbf{q}_{\beta_i,d(i)}$, where $d(i)$ is the direction associated with the i-th sample and each direction **x**, **y**, and **z** is used m times for each run, making a total of $n = 3m$ samples per run. Additionally, the number of positive and negative values for α_i or β_i differed by at most 1 for a given axis, as a way to ensure some variety of estimated attitudes.

As described at the end of Sec. 3.2, the sign constraint on β_i shown in Eq. (5) may cause problems for the algorithm due to noise. To test this effect, two datasets were used to evaluate the algorithm's performance. The first set, named D1, defines an interval $I_\beta = [-\pi, \pi)$, so that β_i can have any value, even if it decreases performance. The second one, named D2, defines an interval $I_\beta = \left[-\frac{3\pi}{4}, -\frac{\pi}{4}\right) \cup \left[\frac{\pi}{4}, \frac{3\pi}{4}\right)$, thus forbidding β_i to be in a range of $\frac{\pi}{4}$ from the regions where it changes sign. For D1 and D2, the rotations were sampled from a uniform distribution over their respective I_β, that is, $\beta_i \sim \mathcal{U}(I_\beta)$.

Once determined each quaternion, the real attitudes $^i\mathbf{q}_{\mathcal{I}}^{\mathcal{S}}$ were computed using Eq. (1). Each sample was also subject to noise to simulate errors from the algorithm used for attitude estimation, which can provide noisy estimates due to measurement noise. The noise was created using a random quaternion given by Eq. (8), which can be written as $^i\mathbf{q}_{\alpha_i,\mathbf{v}_i}^{n}$ according to Eq. (2), and multiplying the angle by a factor $\gamma \leq 1$ to reduce the noise level, obtaining the noise quaternion $^i\mathbf{q}_{\gamma\alpha_i,\mathbf{v}_i}^{n}$, thus describing a noise be composed of a rotation up to $\gamma\pi$ in a random direction. Then this noise quaternion is multiplied by the correct attitude to obtain the attitude estimate $^i\hat{\mathbf{q}}_{\mathcal{I}}^{\mathcal{S}} = {^i\mathbf{q}}_{\gamma\alpha_i,\mathbf{v}_i}^{n} \otimes {^i\mathbf{q}}_{\mathcal{I}}^{\mathcal{S}}$ used in Alg. 1. As the noise was the same for all samples, the weights w_i were considered equal.

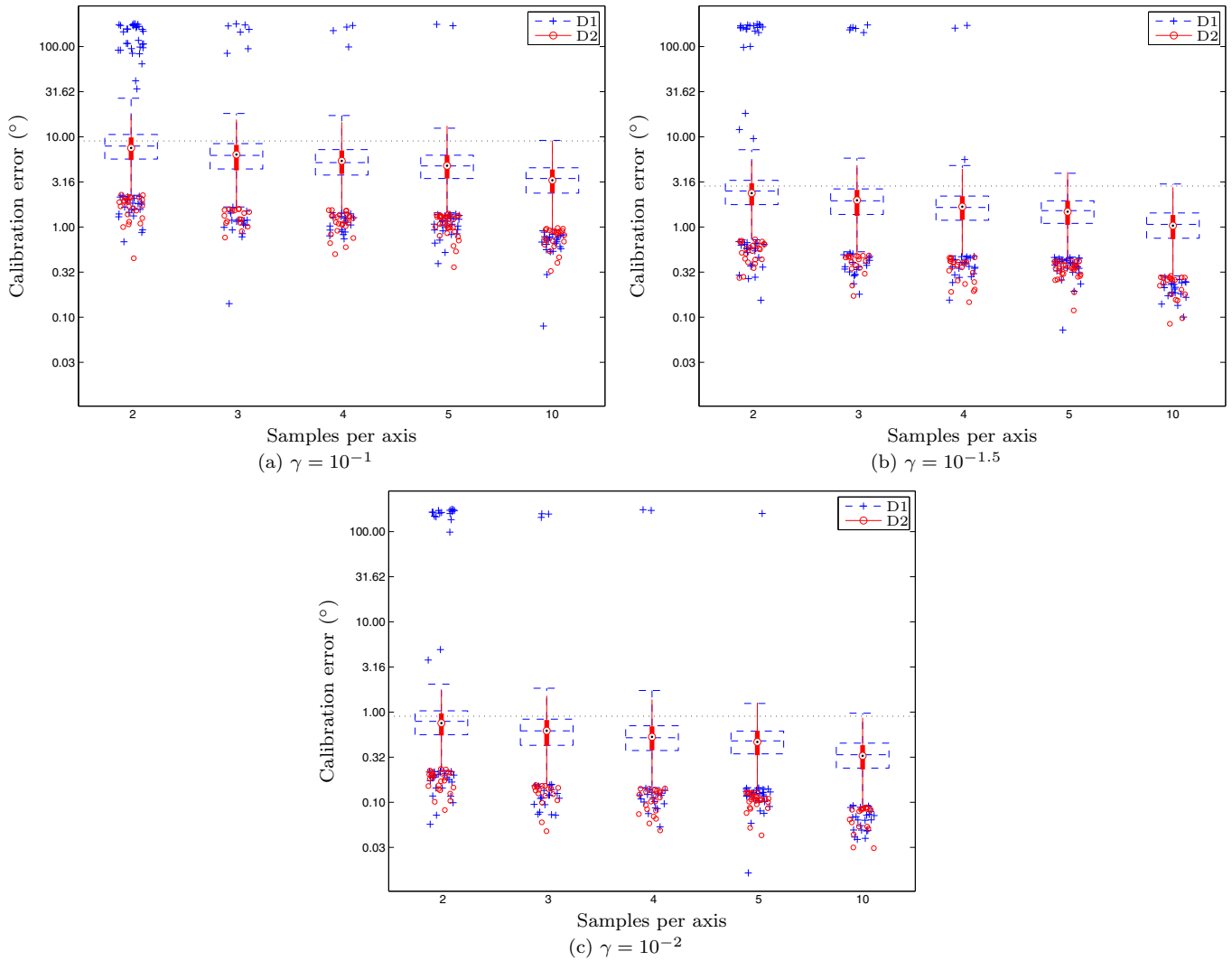Table 1 provides a summary of the parameters used in the simulation.

Fig. 2. Calibration error θ for dataset D1 and D2, with varying noise level and number of attitudes measured for each axis. The median for each noise level is shown by a dotted line.

5.2 Simulation results

After the calibration, the estimate $\hat{\mathbf{q}}_{\mathcal{B}}^{\mathcal{S}}$ is compared to the true value $\mathbf{q}_{\mathcal{B}}^{\mathcal{S}}$. Let the quaternion error be given by

$$\mathbf{q}^{\epsilon} = \hat{\mathbf{q}}_{\mathcal{B}}^{\mathcal{S}} \otimes \left(\mathbf{q}_{\mathcal{B}}^{\mathcal{S}}\right)^{-1}$$

and let q_0^{ϵ} be its scalar component, assumed positive without loss of generality. From Eq. (2), the angle between $\hat{\mathbf{q}}_{\mathcal{B}}^{\mathcal{S}}$ and $\mathbf{q}_{\mathcal{B}}^{\mathcal{S}}$ is given by

$$\theta = 2 \arccos\left(q_0^{\epsilon}\right).$$

Figure 2 shows the errors obtained for D1 and D2 and a variate of values for γ and m. In each figure, the noise's median, given by $\frac{\gamma\pi}{2}$, is shown as a dotted black line for comparison. As can be noted, the algorithm's median error is always below the noise's median, showing that it can correctly merge the information provided by the samples to provide an improvement in the calibration.

As discussed in the end of Sec. 3.2, the choice to change the sign of β_i as a solution to satisfy the inequality restriction must be taken into account during data collection. For D1, where β_i can assume any value, the estimation error is large for some cases when m is small. In these cases,

the number of samples isn't able to compensate for the increase in cost due to the sign change, so the algorithm looks for other ways to reduce the total cost in Eq. (5) and ends up increasing the calibration's error for the desired rotation between body and sensor frames. However, for larger values of m, the presence of more samples reduces the relative cost of an error in β_i and provides more evidence for the correct rotation, leading to more precise estimates.

For D2, where the values of β_i are restricted to regions where the noise won't change the sign of its best fit, no such problem occurs for any m and γ, and the estimate is always close to the correct value. Moreover, the performance using D2 is similar to using D1, even though it has lower diversity on its samples.

If an upper bound for the noise level of the attitude estimates and orientation error is known, the restriction on ranges for β_i can be properly adjusted to prevent large estimation errors by avoiding regions where the sign provided through $s(i)$ may become inconsistent with the attitude estimate. If the noise level is unknown, results show that the algorithm will converge to values similar

to the restricted case if enough samples are provided, establishing a trade-off between the number of samples needed for an adequate calibration and the confidence that the signs provided through $s(i)$ are consistent with the attitude estimates.

6. CONCLUSION

This paper presented a calibration algorithm to estimate the rotation between the sensor and body frames based on the quaternion averaging problem. The algorithm depends only on attitude estimates and minimal user input, thus being easy to use and compatible with any attitude estimation algorithm the system may already have.

Using noisy synthetic data, the algorithm was able to achieve estimates close to the real values in most cases, even though the optimization problem has many more degrees of freedom than only the desired rotation, due to the usability constraint that imposes less restrictions on the user, and its objective is different from the calibration one, although they are related. For any number of samples, the error median is below the noise median, showing it was able to filter out part of the noise, and the error decreases as more samples are provided. Furthermore, the conditions in which the algorithm may perform poorly were described and a solution to avoid such cases was tested successfully, showing that a more strict methodology during the attitude sampling allows the user to avoid low-quality estimates. This methodology creates a trade-off between user knowledge about the system and the number of samples required for proper calibration.

This trade-off occurs because the information provided by the user may be inconsistent with the attitude estimates due to estimation errors, which in turn leads to a constraint in the problem not being satisfied. Two solutions to this problem are discussed, both having significant but distinct disadvantages. If a hybrid solution, that is able to detect when the constraint is violated only because of attitude estimates' noises and correctly choose the appropriate way to satisfy the constraint, is found, then the user may always follow the simplified data capture method. Furthermore, such method may even decrease the error for the cases the current one already works.

Another, possibly much simpler but not as effective, solution would be to detect whether the error would be excessively high. This could be achieved, for instance, by an error predictor, which estimates the calibration error given the estimated quaternions. However, such predictor may not exist, so another possibility is to compare the solutions obtained from subsets of samples, which allows comparison between rotations that should have similar values.

Finally, the algorithm is currently being validated using real sensors, and preliminary results show that the performance obtained in simulation is similar to the one obtained with experimental data, hence future work will include experiments, not only simulations.

REFERENCES

Alonso, R. and Shuster, M.D. (2002). Complete linear attitude-independent magnetometer calibration. *Journal of the Astronautical Sciences*, 50(4), 477–490.

Batista, P., Silvestre, C., and Oliveira, P. (2009). Sensor-based complementary globally asymptotically stable filters for attitude estimation. In *Proceedings of the IEEE Conference on Decision and Control*, 7563–7568. IEEE.

Elkaim, G.H. (2013). Misalignment calibration using body frame measurements. In *American Control Conference*. IEEE.

Elkaim, G.H., Lie, F.A.P., and Gebre-Egziabher, D. (2012). Principles of guidance, navigation and control of UAVs. Technical report.

Gebre-Egziabher, D., Elkaim, G.H., Powell, J.D., and Parkinson, B.W. (2000). A gyro-free quaternion-based attitude determination system suitable for implementation using low cost sensors. In *Position Location and Navigation Symposium*, 185–192. IEEE.

Kuffner, J.J. (2004). Effective sampling and distance metrics for 3D rigid body path planning. In *Proceedings of the IEEE International Conference on Robotics and Automation*, April, 3993–3998, vol. 4. IEEE.

Le, Q.V. and Ng, A.Y. (2009). Joint calibration of multiple sensors. In *Proceedings of the IEEE International Conference on Intelligent Robots and Systems*, 3651–3658. IEEE.

Madgwick, S.O.H., Harrison, A.J.L., and Vaidyanathan, R. (2011). Estimation of IMU and MARG orientation using a gradient descent algorithm. In *Proceedings of the IEEE International Conference on Rehabilitation Robotics*, 1–7. IEEE.

Mahony, R., Hamel, T., and Pflimlin, J.M. (2008). Nonlinear complementary filters on the special orthogonal group. *IEEE Transactions on Automatic Control*, 53(5), 1203–1218.

Markley, F.L., Cheng, Y., Crassidis, J.L., and Oshman, Y. (2007). Averaging quaternions. *Journal of Guidance, Control, and Dynamics*, 30(4), 1193–1197.

Miranda, C.S. and Ferreira, J.V. (2013). Greedy calibration of the rotation between sensor and body frame without external references. In *Proceedings of the ABCM International Congress of Mechanical Engineering*. ABCM.

Sabatini, A.M. (2006). Quaternion-based extended Kalman filter for determining orientation by inertial and magnetic sensing. *IEEE Transactions on Biomedical Engineering*, 53(7), 1346–1356.

Schopp, P., Klingbeil, L., Peters, C., and Manoli, Y. (2010). Design, geometry evaluation, and calibration of a gyroscope-free inertial measurement unit. *Sensors and Actuators A: Physical*, 162(2), 379–387.

Shuster, M. (2006). The generalized Wahba problem. *Journal of the Astronautical Sciences*, 54(2), 245–259.

Thrun, S., Burgard, W., and Fox, D. (2005). *Probabilistic robotics*. Intelligent Robotics and Autonomous Agents Series. Mit Press.

Vasconcelos, J.F., Elkaim, G.H., Silvestre, C., Oliveira, P., and Cardeira, B. (2011). Geometric approach to strapdown magnetometer calibration in sensor frame. *IEEE Transactions on Aerospace and Electronic Systems*, 47(2), 1293–1306.